Gümüşhane University Journal of Science and Technology

GUFBD / *GUJS* (2026) 16(2): 617-635 doi: 10.17714/gumusfenbil.1856976 Research Article

PVA/Agar based films reinforced with pickering emulsion of *Achillea millefolium* L. essential oil

Nuh Yasin YILDIZ[1], **Begüm ATARDİKER**[1], **Simge OĞUZ**[1], **Efsun ECEVİT**[1] **Ayşenur YEŞİLYURT***[1]

[1]*Department of Chemical Engineering, Faculty of Engineering and Natural Sciences, Bursa Technical University, 16310, Bursa, Türkiye*

• Received: 05.01.2026 • Accepted: 05.06.2026

Abstract
Wound dressings play a critical role in accelerating the healing process by reducing infection risk and maintaining a moist environment. In this study, biodegradable poly(vinyl alcohol) (PVA)/agar films were prepared for wound care applications. *Achillea millefolium* L. essential oil (AMO) was extracted by steam distillation and incorporated at 0.5–5 % (v/v) using a β-cyclodextrin-stabilized Pickering emulsion. At low loadings, polymer additive interactions were enhanced through hydrogen bonding; in particular, the PA-AMO1 film (1 % v/v) showed the best performance, with a tensile strength of 11.3 MPa and elongation at break of 719 %. Increasing AMO content raised the total color difference and yellowness index. Contact angle measurements indicated more hydrophobic surfaces, while all films remained overall hydrophilic. Antibacterial assays demonstrated concentration-dependent inhibition against *Escherichia coli* (*E. coli*, up to 18.5 mm at 5 % AMO), whereas no activity was detected against *Staphylococcus aureus* (*S. aureus*). In conclusion, PVA/Agar films prepared via β-cyclodextrin-assisted AMO encapsulation, especially PA-AMO1 exhibited optimal mechanical and surface performance, with higher AMO imparting selective antibacterial activity. These results highlight AMO-loaded PVA/Agar films as promising wound dressing candidates.

Keywords: Agar, Achillea millefolium L. essential oil, Pickering emulsion, Polyvinyl alcohol (PVA), Wound dressing

1. Introduction

The skin, the body's largest organ, acts as the main and most vital protective barrier against external conditions (Vig et al., 2017; Tavakoli & Klar, 2020; Uberoi et al., 2024). However, various factors such as physical trauma (injuries, chemical abrasions) or diseases (microbial infections, metabolic disorders) can compromise skin integrity and lead to the formation of wounds (Russo et al., 2020; Blackburn et al., 2024; Lei et al., 2025). The healing of skin wounds is a complex, interrelated, three-phase regenerative process: initially hemostasis and inflammation occur, followed by proliferation (cell growth and tissue formation), and finally remodeling (tissue reorganization and maturation) (Martin, 1997; Peña & Martin, 2024; Cavallo et al., 2024; Yan et al., 2025). Any disruption of these sequential stages can delay or impair healing, potentially resulting in acute or chronic wounds (Egri & Erdemir, 2019; Buriti et al., 2024).

Although wounds possess a natural self regeneration capability, wound dressings are of paramount importance for accelerating the healing process and reducing the risk of infection (Buriti et al., 2024; Baladi & Sherafat, 2025). Effective dressings should isolate the wound, maintain physiological temperature, preserve moisture balance while absorbing wound exudates, and allow gas exchange for oxygen permeability (Athamneh et al., 2023). In addition, ideal wound dressings are expected to possess low toxicity, be derived from sustainable sources, ensure optimal gas and water vapor permeability, be easily removable, combine flexibility with sufficient mechanical strength, and remain cost-effective (Tyeb et al., 2018).

To meet these requirements, wound dressing materials have been developed in various forms, including films, foams, hydrogels, hydrocolloids, and alginates, with polymer-based systems being the most common

*Ayşenur YEŞİLYURT; aysenur.erdogan@btu.edu.tr

(Buriti et al., 2024). These polymers may be of natural or synthetic origin. Natural polymers such as chitosan, collagen, alginate, agar, and hyaluronic acid are biocompatible and biodegradable, while synthetic polymers such as polyamides (e.g., nylons, PA), polyvinyl alcohol (PVA), polytetrafluoroethylene (PTFE), polyvinyl chloride (PVC), and polyisoprene (PI) are also widely used (Buriti et al., 2024; Baladi & Sherafat, 2025; Lei et al., 2025). Natural and synthetic polymers are attractive because their degradation rate, mechanical strength, and pore structure can be engineered, and they can be processed into forms possessing high surface area to volume ratios (Buriti et al., 2024).

PVA is formed via the hydrolytic conversion of vinyl acetate and consists of repeating ethylene oxide derived (C_2H_4O) units (Khorasani et al., 2021; Jin, 2022). This polymer is transparent, odorless, and easily soluble in water (Cao et al., 2021), and its molecular weight varies as a function of the degree to which hydrolysis proceeds (Jin, 2022). PVA exhibits excellent biocompatibility, biodegradability, non-toxicity, high tensile strength, superior flexibility, easy processability, and relatively good thermal resistance, thereby making it a valuable candidate for biomedical applications (Chen et al., 2018; Teodorescu et al., 2018; Chen et al., 2019; Sang Su Ha, 2020; Pérez-Nava et al., 2023). Its abundance of hydroxyl (–OH) groups confers high hydrophilicity, enabling hydrogen bonding with biomolecules and thus supporting cell adhesion and proliferation. This hydrophilicity also enhances water absorption and provides a moist environment, which is vital for cell viability and tissue regeneration (Xiang et al., 2024). Furthermore, its elasticity, which resembles that of human tissue, combined with its outstanding mechanical strength, allows PVA to be used to enhance the performance of other materials (Zhou et al., 2021).

Due to these superior attributes, PVA has emerged as a potential polymeric material for the fabrication of biopolymer based films intended for biomedical purposes (Feng et al., 2021). Chemically cross-linked PVA based films preserve their integrity against dissolution while their network structures allow significant water absorption and swelling. This high water uptake capacity creates a moist environment, facilitates the absorption of excess wound exudates, and promotes cell growth and repair, making them suitable candidates for applications such as wound dressings and drug delivery (Lohakan et al., 2010; Brumberg et al., 2021). PVA is widely used in wound dressing applications due to its favorable physicochemical and biological properties. However, PVA itself does not possess significant intrinsic antibacterial activity, which limits its effectiveness in preventing microbial growth when used alone. Previous studies have consistently reported that PVA-based materials exhibit weak or negligible antibacterial performance, thereby requiring modification with bioactive agents (Fang et al., 2019; Tamer et al., 2021; Li et al., 2022).

To overcome this limitation, PVA is commonly combined with antibacterial compounds such as plant-derived molecules, nanoparticles, or antibiotics, which confer the required antimicrobial functionality to the system (Li et al., 2022; Gu et al., 2025). These approaches enable the retention of PVA's biocompatibility and mechanical advantages while improving its antibacterial performance for wound healing applications.

Similarly, agar contains abundant hydroxyl groups, which can interact with PVA chains and restrict the solubility of the films in water. Therefore, agar is considered a good candidate to improve the hydrophobicity of highly hydrophilic PVA (Pham et al., 2021). Agar is a natural hydrocolloid extracted from red seaweeds (Rhodophyta) (Reddy & Rhim, 2014). Its polysaccharide structure consists of two main components: agarose and agaropectin. One of the most distinctive features of agar is its insolubility at room temperature, whereas it dissolves upon heating to ~90 °C. Upon cooling, agarose chains form helical structures that produce a thermo-reversible gel network (Gasperini et al., 2014; Giulio Fittolani, 2019). Its non-toxic and non-irritant nature, biodegradability, biocompatibility, and ability to form gels without external cross-linkers make agar a safe material for applications in food, cosmetics, and biomedical sectors (Arham, 2016; Gioele et al., 2017; Abdul Khalil et al., 2018).

The polymers used in this study lack intrinsic antibacterial or antimicrobial activity. In modern wound dressings, the incorporation of plant-derived essential oils (EO) with antimicrobial properties has been shown to support hemostasis, inflammation, collagen synthesis, and epithelialization during the healing process (Egri & Erdemir, 2019).

Achillea millefolium L. (AML) or yarrow is a medicinal plant that has been traditionally used for centuries. According to historical records, ancient Greeks employed this plant to treat injured soldiers in battle, and the legendary warrior Achilles is said to have derived his name from it. Dioscorides also documented the potent biological effects of AML (Wendy L. Applequist, 2011; Mohammadhosseini et al., 2017). Traditionally, it has been used internally for headaches, digestive, and liver disorders, and externally for burns, cuts, wounds, and inflammations (Ali et al., 2017). In the European Union Cosmetic Ingredients Inventory (CosIng), AML extract is defined as a tonic, cleanser, and skin-conditioning agent, and is regarded as a safe component (Becker et al., 2016; Czech et al., 2023). Its popularity in skin-health formulations is attributed to its complex mixture of secondary metabolites, including phenolic compounds like apigenin and caffeoylquinic acid derivatives, terpenes such as camphor and linalool, phytosterols like β-sitosterol and stigmasterol, as well as numerous fatty acids (Ali et al., 2017; Strzepek-Gomolka et al., 2021). In addition, GC–MS analyses of *Achillea millefolium* essential oil have revealed a complex composition consisting of numerous monoterpene and sesquiterpene compounds. The major constituents include (+)-2-bornanone (35.15%), eucalyptol (30.80%), sabinene (5.57%), α-terpineol (5.07%), camphene (4.22%), and copaen-4-α-ol (3.43%), which collectively account for a significant proportion of the total oil (Nazir et al., 2022). In addition, 1,8-cineole (eucalyptol) has been consistently reported as a dominant oxygenated monoterpene, typically ranging between 10% and 34% depending on the study (Tuberoso & Kowalczyk, 2009; Farhadi et al., 2020). Other monoterpenes such as sabinene, α-terpineol, and terpinen-4-ol, as well as sesquiterpenes including germacrene D, β-caryophyllene, and chamazulene, have also been identified as key constituents of the essential oil (Verma et al., 2017; Pulaj et al., 2024). The relative abundance of these compounds varies significantly depending on geographical origin, environmental conditions, and the phenological stage of the plant. Therefore, the chemical profile of *Achillea millefolium* L. essential oil exhibits considerable variability, which plays a critical role in determining its biological activities. In recent years, studies have further revealed its broad-spectrum antimicrobial activity. Extracts obtained using solvents such as ethanol, water, and hexane show antimicrobial activity against a variety of pathogens, encompassing Gram-positive bacteria (*S. aureus*), multiple Gram-negative species (e.g., *E. coli*, *K. pneumoniae*, *P. aeruginosa*, *S. enteritidis*), and opportunistic fungi like *A. niger* and *C. albicans* (Stojanovic et al., 2005; Villalva et al., 2022). Notably, its essential oil has shown strong antimicrobial activity against pathogenic bacteria such as *S. aureus* and *S. Typhimurium* (Verma et al., 2017).

In this study, biodegradable wound dressing films based on PVA/Agar were prepared using a Pickering emulsion approach. β-cyclodextrin (β-CD) was employed as a stabilizer for the Pickering emulsion, thereby enabling homogeneous encapsulation and integration of *Achillea millefolium* L. essential oil (AMO) into the polymer matrix. The effects of the β-CD/AMO inclusion complex on the polymer matrix were comprehensively evaluated in terms of morphological, physical, biological, and chemical properties. Beyond these functional performances, the utilization of biodegradable polymers and a plant-derived essential oil also emphasizes the sustainability of this approach, highlighting its potential to contribute to environmentally friendly and bio-based wound care solutions.

2. Material and method

2.1. Materials

PVA granules (87–89 % hydrolyzed, Kuraray, Osaka, Japan) and agar powder (Tunalı Group Gıda Kozmetik Ltd. Şti., Istanbul, Türkiye) were used as polymeric raw materials. *Achillea millefolium* L. was procured from a local market in Bursa, Türkiye. β-Cyclodextrin was purchased from AFG Bioscience (Northbrook, IL, USA). Glycerol (99.5 % purity, Tekkim, Istanbul, Türkiye) and citric acid (99.5 % purity, Merck, Darmstadt, Germany) were obtained from commercial suppliers.

2.2. Extraction of *Achillea millefolium L.* essential oil

Washed and finely chopped *Achillea millefolium* L. samples were processed by hydrodistillation using a standard Clevenger apparatus. The extraction mixture was prepared by adding plant material and distilled water in a 1:10 (w/v) proportion, and the suspension was boiled for 3 h. The volatile oil released with steam was condensed and collected in the graduated Clevenger arm. The essential oil was separated from the aqueous phase using a separating funnel. The essential oil yield of *Achillea millefolium* was determined as 0.4% under the applied extraction conditions. This value falls within the range commonly reported in the literature (0.1–0.7%), indicating consistency with previously published studies (Verma et al., 2017; Nazir et al., 2022). The oil was obtained without any solvent, stored in light-resistant bottles, and preserved at 4 °C until further use.

2.3. Preparation of PVA/Agar based films for wound dressing applications

To prepare biodegradable films, 9.0 g of PVA granules and 1.5 g of agar powder were separately dissolved in distilled water at 90 °C until complete dissolution and homogeneity were achieved, and the final volume of each solution was adjusted to 100 mL. The two solutions were then combined at a 90/10 (v/v) ratio and magnetically stirred for 2 h to obtain a uniform mixture. Glycerol (as a plasticizer), citric acid (as a cross-linker), and β-cyclodextrin (as an emulsifier) were added at the proportions listed in Table 1, each with a 1 h interval. The mixture was further stirred overnight, and on the following day, AMO was incorporated at different concentrations (0.5%, 1%, 2%, and 5%, v/v). A control film without essential oil was prepared as a reference sample. All casting solutions were poured into 12 cm Petri dishes and dried at 25 °C in a regulated oven until solvent removal was complete.

Table 1 lists the individual quantities of polymer, plasticizer, cross-linker, emulsifier, and essential oil used in each sample, whereas Figure 1 offers a schematic depiction of the film production process.

2.4. Characterization of the wound healing films

The chemical structure of the prepared films was analyzed using a PerkinElmer Spectrum Two FT-IR spectrophotometer equipped with a diamond ATR accessory. Measurements were performed in ATR mode with a resolution of 4 cm^{-1}, averaged over 16 scans, and recorded in the range of 4000–400 cm^{-1}.

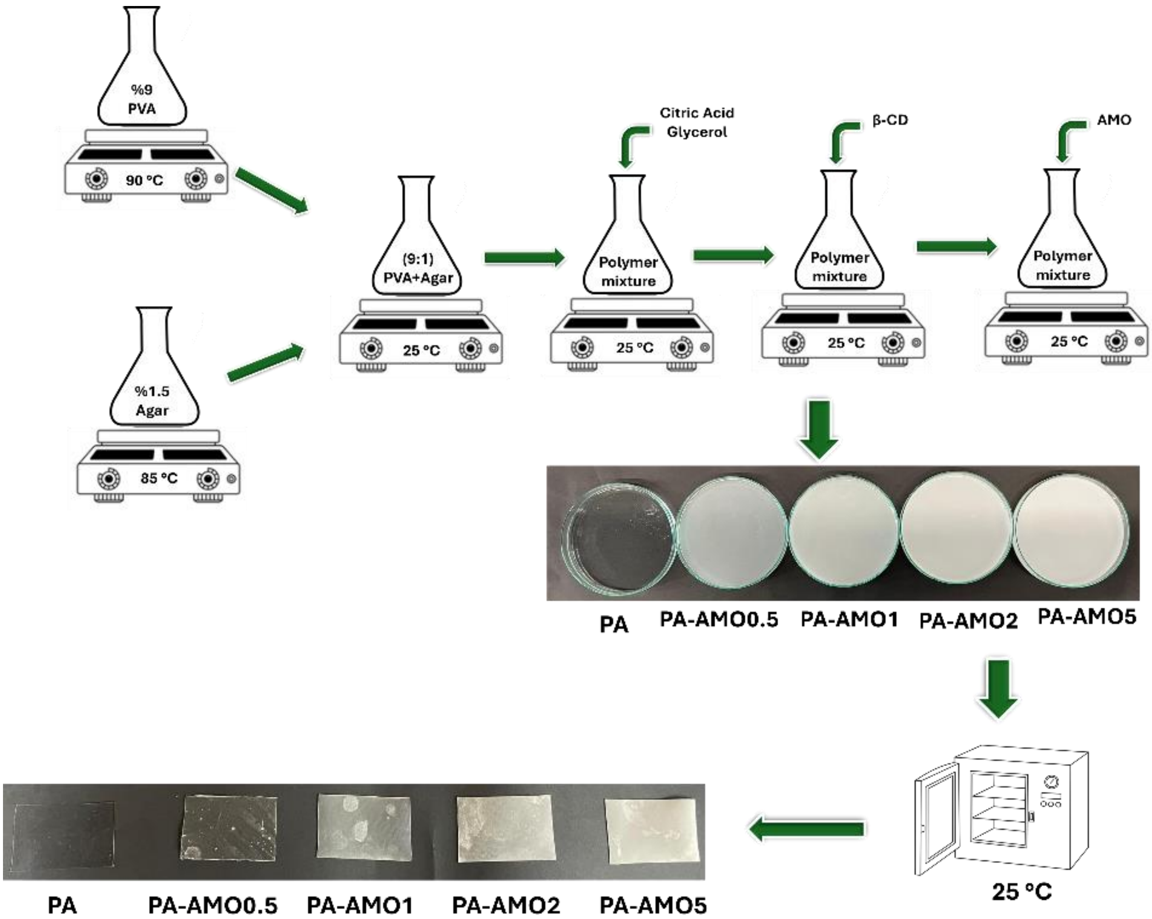

Figure 1. Schematic representation of the preparation process of PVA/Agar based films enriched with *Achillea millefolium* L. essential oil.

The surface and cross-sectional morphologies of the films were examined with a Carl Zeiss/Gemini 300 scanning electron microscope (SEM). Prior to SEM observation, the film samples were sputter-coated with a thin Au/Pd layer (~10–15 nm) using a Leica/ACE600 coater to enhance electron conductivity. The analyses were conducted at an accelerating voltage of 5 kV, and images were captured at magnifications between 250× and 500×.

Thickness measurements were obtained for each film by acquiring three readings from randomly selected positions with a digital caliper (Macrona, Türkiye). The final thickness for each sample was expressed as the arithmetic mean of these measurements.

Table 1. Formulations of the PVA/Agar based composite films.

Sample ID	PVA (% v/v)	Agar (% v/v)	AMO (% v/v)	β -CD (% w/v)	Citric acid (% v/v)	Glycerol (% v/v)
PA	90	10	0	0	1.50	1.30
PA-AMO0.5	90	10	0.15	0.15	1.50	1.30
PA-AMO1	90	10	0.30	0.30	1.50	1.30
PA-AMO2	90	10	0.60	0.60	1.50	1.30
PA-AMO5	90	10	1.20	1.20	1.50	1.30

Mechanical characterization followed ASTM D882-18, which outlines the procedure for evaluating tensile properties of thin plastic films. Tests were performed using a Shimadzu AGS-X universal testing machine (1 kN load cell, Japan). Conditioning of the specimens was carried out for no less than 40 h at 23 °C and 50% RH in accordance with ASTM D618 (Procedure A). Film samples were prepared as strips 1.0 cm in width with an effective gauge length of 50 mm, and tensile measurements were conducted at a controlled crosshead speed of 25 mm/min. Tensile strength, young's modulus, and elongation at break were measured in five repetitions, with results presented as mean values accompanied by standard deviations.

Color measurements were carried out on film specimens (2×2 cm) using a Konica Minolta spectrophotometer (D65 standard daylight). The instrument was calibrated with a standard white reference plate (L^*: 93.74 ± 0.05, a^*: 2.22 ± 0, b^*: −12.71 ± 0.11) prior to analysis. Five measurements were performed on different areas of each sample, and the L, a, and b color coordinates were recorded. Results were reported as mean ± standard deviation.

The total color difference (ΔE) was computed as the overall numerical disparity between the sample's color coordinates and those of the reference. Lower ΔE values indicate closer similarity to the reference, while higher ΔE values represent more pronounced visual differences. The yellowness index (YI) and ΔE were calculated according to Equations (1) and (2).

$$YI = \frac{b}{L} * 142.86 \quad (1)$$

$$\Delta E = \sqrt{(L - L^*)^2 + (a - a^*)^2 + (b - b^*)^2} \quad (2)$$

In this color space, L quantifies the degree of lightness of the film, while a specifies its coloration between red and green, with positive numbers signifying a red tendency and negative numbers a green tendency. The b coordinate describes the position along the yellow–blue axis, where positive values correspond to yellowish tones and negative values indicate increased blueness.

Wettability analysis was conducted by recording static contact angles with an Attension Theta Lite instrument. Distilled water droplets were applied to 2 × 2 cm samples, and angles were computed via the sessile-drop method using Young–Laplace fitting. The mean contact angle for each specimen was calculated from the left and right droplet interfaces.

The antimicrobial effects of the developed films were investigated by employing a standard disk diffusion procedure. Two bacterial species were selected to represent Gram-negative (*E. coli*, ATCC 25922) and Gram-positive (*S. aureus*, ATCC 10832) groups. Frozen bacterial stocks maintained at −20 °C in 16% glycerol were streaked on Mueller Hinton agar and incubated at 37 °C for 16–24 h, after which morphologically uniform colonies were transferred to Mueller Hinton broth and adjusted to the 0.5 McFarland turbidity standard (approximately 10^8 CFU/mL). The film samples were sterilized under UV irradiation for 30 min and positioned on agar plates seeded with the standardized cultures. Plates were incubated at 37 °C for 16–24 h, and inhibition zones were quantified using calipers as the complete diameter surrounding the film. All measurements were performed in duplicate.

2.5. Statistical analysis

Mechanical and colorimetric data were subjected to statistical evaluation using IBM SPSS Statistics v22. Results were expressed as mean ± standard deviation. One-way analysis of variance (ANOVA) was performed to evaluate differences among groups, and Tukey's HSD post hoc test was applied to determine significant differences. A significance threshold of $p < 0.05$ was adopted for all analyses.

3. Results and discussion

3.1. Chemical composition of the films

FTIR spectroscopy was employed to characterize the functional groups of the polymer constituents and to probe the interactions occurring between the PVA/agar matrix and the *Achillea millefolium* L. essential oil/β-CD complex. Representative ATR-FTIR spectra of the pristine PA film and the AMO-containing films are shown in Figure 2. The spectra of PA exhibit the expected absorption features of PVA and agar, confirming the presence of their characteristic vibrational modes. The broad band centred near 3268 cm^{-1} is associated with O–H stretching vibrations of hydroxyl groups from both PVA and agar and appears broadened due to extensive intermolecular hydrogen bonding (Mansur et al., 2008). The signals at approximately 2914 and 2886 cm^{-1} arise from the stretching of methylene ($–CH_2$) groups. The peak detected around 1719 cm^{-1} corresponds to C=O stretching of residual acetate groups from partially hydrolyzed poly(vinyl acetate) segments in PVA. The band observed near 1426 cm^{-1} originates from aliphatic C–H bending, while the feature at about 1256 cm^{-1} is attributed to asymmetric C–O–C stretching of ester or glycosidic linkages (Yesilyurt, 2025). The region spanning 1166–1091–1015 cm^{-1} encompasses C–O–C and C–O vibrations characteristic of PVA and polysaccharides, with the absorption around 1140–1160 cm^{-1} being particularly responsive to variations in PVA crystallinity (Liang et al., 2024). The peak at roughly 845 cm^{-1} reflects the skeletal C–O–C vibrations of 3,6-anhydrogalactose units present in agar (Fernando et al., 2017).

Incorporation of the AMO/β-CD complex did not introduce new bands, and the spectra closely resembled those of the neat PA films, indicating the absence of covalent bond formation. Nonetheless, subtle shifts and broadening observed in the O–H stretching region imply modified hydrogen-bonding interactions between the polymer matrix and the AMO/β-CD complexes, supporting their effective integration into the film structure.

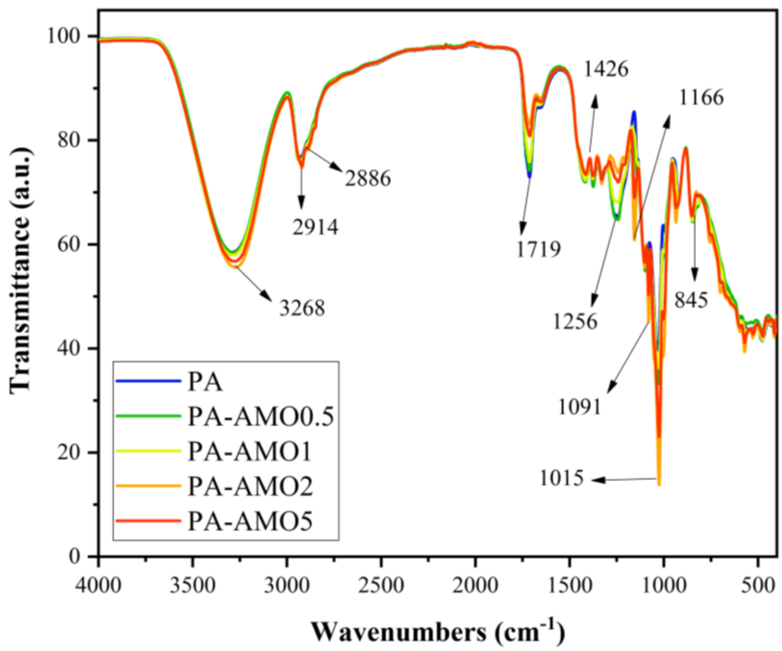

Figure 2. FTIR spectra of neat PA and AMO/β-CD incorporated wound healing films.

3.2. Film cross-section and surface morphology (SEM)

SEM analysis revealed the microstructure of the wound healing film surfaces and cross-sections, enabling the correlation between morphology and macroscopic properties. Figure 3 presents SEM micrographs of the film samples. As shown in Figures 3a–3b, the neat PVA/Agar film exhibited a highly homogeneous morphology with only a limited number of microcracks. This uniform structure indicates good compatibility between PVA and agar polymers.

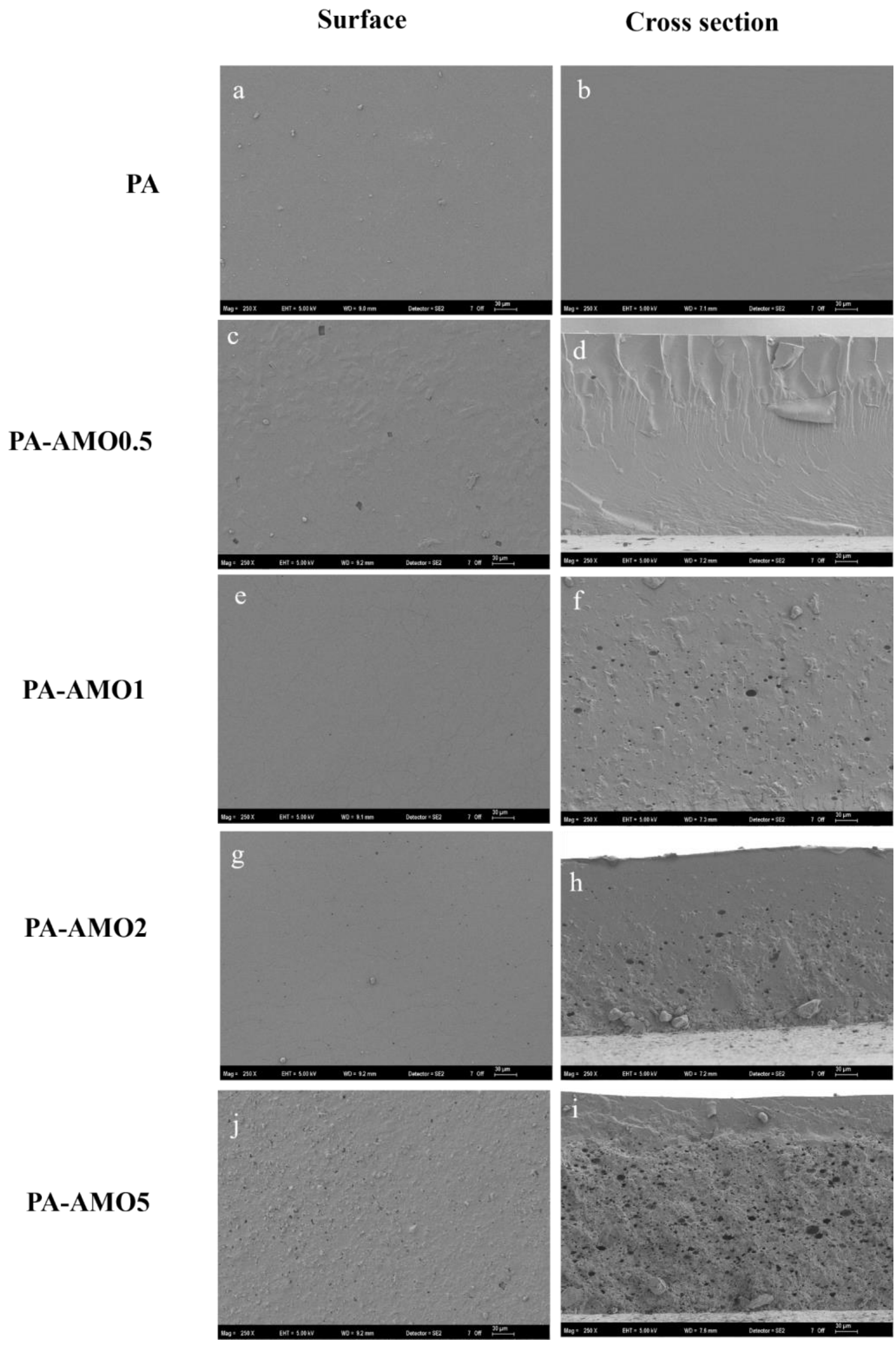

Figure 3. SEM micrographs of the surface (a, c, e, g, j) and cross-section (b, d, f, h, i) of PVA/Agar based films enriched with *Achillea millefolium* L. essential oil.

With the incorporation of *Achillea millefolium* L. essential oil, distinct morphological changes were observed in the film surfaces and cross-sections. Increasing essential oil concentrations reduced the surface smoothness, leading to the formation of microcracks and Pickering emulsion droplets. Such irregularities may be attributed to emulsion flocculation during the drying process or the upward migration of oil droplets toward the film surface during solvent removal (Almasi et al., 2020). Similarly, Liu et al. (Liu et al., 2019) reported that increasing amounts of essential oil in films resulted in irregularities and porous structures in the SEM micrographs.

Morphological changes are of particular importance in terms of the potential use of the films as wound dressings. Homogeneous structures can better adapt to the wound surface, thereby enhancing the barrier function, while heterogeneous regions formed due to essential oil incorporation may facilitate the controlled release of the oil. Thus, morphological features contribute not only to the mechanical strength of the films but also directly to their biological performance.

3.3. Wettability of film surfaces

Static contact angle measurements were performed to characterize the surface behavior of the wound-healing films and to determine whether the materials exhibited hydrophilic or hydrophobic tendencies. In general, surfaces with a contact angle < 90° are regarded as hydrophilic, whereas values > 90° reflect hydrophobic characteristics. A reduction in contact angle corresponds to enhanced surface wettability (El-Aassar et al., 2020). The water contact angles obtained for the PA, PA-AMO0.5, PA-AMO1, PA-AMO2, and PA-AMO5 films are summarized in Table 2 and depicted in Figure 4.

Table 2. Contact angle values and inhibition-zone diameters of the films.

Sample ID	Contact Angle* (°)	*E. coli* (mm)	*S. aureus* (mm)
PA	45.01 ± 1.78^{a}	14±0	-
PA-AMO0.5	56.72 ± 0.93^{b}	12.5±0.5	-
PA-AMO1	63.45 ± 1.34^{c}	-	-
PA-AMO2	65.74 ± 0.73^{c,d}	16±0	-
PA-AMO5	63.12 ± 2.69^{c}	18.5±0.5	-

*Different superscript letters in each column denote significant differences between groups ($p < 0.05$).

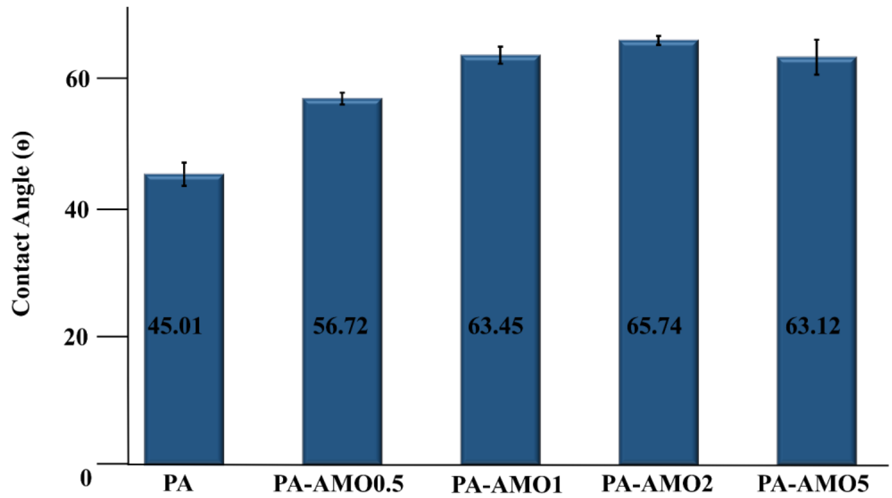

Figure 4. Contact angles of PA, PA-AMO0.5, PA-AMO1, PA-AMO2, and PA-AMO5 films.

The control PA film displayed the smallest contact angle (45.01 ± 1.78°), consistent with the inherently hydrophilic character of PVA and agar, both of which possess abundant surface hydroxyl groups capable of interacting readily with water molecules. Incorporation of the AMO/β-CD complex significantly increased the contact angle, yielding 56.72 ± 0.93° for PA-AMO0.5, 63.45 ± 1.34° for PA-AMO1, 65.74 ± 0.73° for PA-AMO2, and 63.12 ± 2.69° for PA-AMO5.

Multiple comparison analysis confirmed that all AMO/β-CD-containing films exhibited significantly higher contact angles than PA ($p < 0.05$). No statistically significant differences were detected among PA-AMO1, PA-AMO2 and PA-AMO5 ($p > 0.05$). These observations suggest that incorporation of the AMO/β-CD complex decreases the availability of free hydroxyl groups for interaction with water, thereby rendering the film surfaces more hydrophobic. A comparable effect was reported by Karami et al. (2022), who observed that the addition of AMO to gelatin–sodium alginate films reduced surface hydrophilicity and consequently increased the contact angle (Karami et al., 2022).

Nevertheless, the contact angle values of all films remained below 90°, indicating that the surfaces generally retained their hydrophilic character. Hydrophilic surfaces are advantageous for wound healing, as they help restrict bacterial growth while facilitating cell adhesion and proliferation (Yuan et al., 2018; Kharat et al., 2021).

3.4. Antibacterial activities of the films

Antibacterial efficacy is of critical importance in wound dressing materials, as bacterial colonization slows down healing and increases the risk of infection (Negut et al., 2018). Therefore, the activities of the developed films against *S. aureus* and *E. coli* were evaluated using the disk diffusion method. The inhibition zones obtained by the disk diffusion assay are presented in Figure 5. Table 2 compiles the corresponding inhibition-zone diameters against *E. coli* and *S. aureus*.

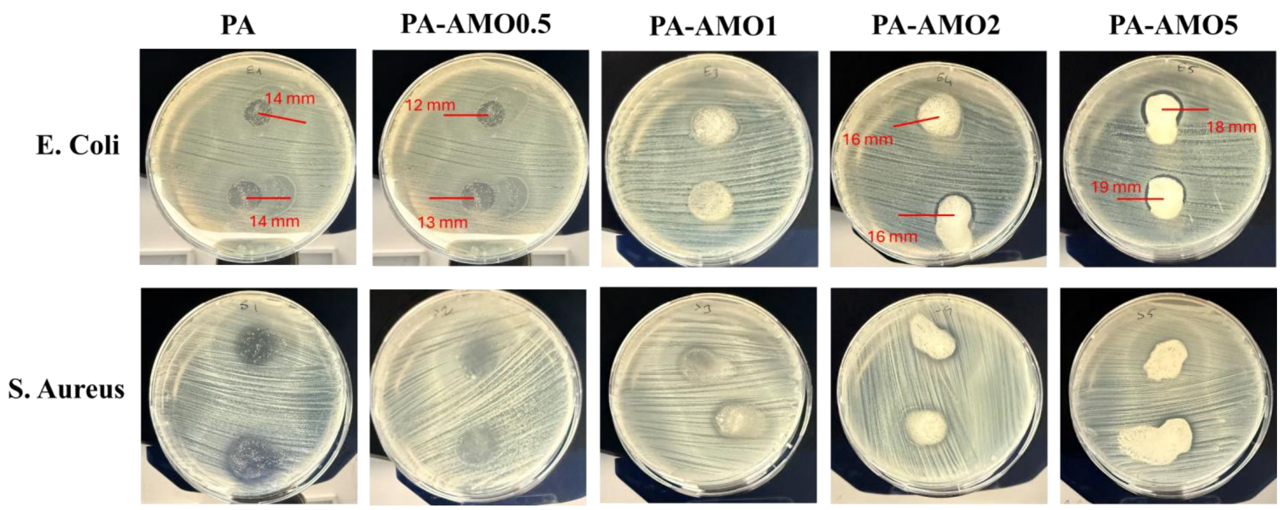

Figure 5. Antibacterial activities of neat PA and AMO-incorporated PA films against *E. coli* and *S. aureus* determined by the disk diffusion method.

For the reference PA and PA-AMO0.5 films, measurable inhibition zones were observed only against *E. coli* (14.0 and 12.5 mm, respectively), whereas no inhibition zones were detected against *S. aureus*. The PA-AMO1 film did not exhibit detectable activity against either bacterium. At higher AMO contents, the antibacterial activity against *E. coli* increased, and the PA-AMO2 and PA-AMO5 films produced inhibition zones of 16.0 and 18.5 mm, respectively, while *S. aureus* remained unaffected. These results indicate that the antibacterial response of the films was not strictly linear with increasing AMO content, since the inhibition observed for the control PA film decreased at low AMO loading and then increased again at higher AMO concentrations. Such non-linear behavior has also been reported in the literature for essential-oil-based antibacterial systems. Ike et al. (2025) showed that essential oil blends may allow bacterial growth at low concentrations, display irregular growth behavior at intermediate concentrations, and completely inhibit growth only at sufficiently high concentrations, indicating that the antibacterial response may fluctuate across the concentration range rather than increase in a strictly proportional manner (Ike et al., 2025).

The antibacterial performance observed here is also consistent with previous studies showing that essential-oil-containing polymer films can exhibit measurable inhibition zones, although the magnitude of the effect depends strongly on the polymer matrix, essential oil type, and release behavior. For example, agar-based films containing savory essential oil were reported to be more effective against Gram-positive bacteria than against *E. coli*, demonstrating that the film matrix can strongly influence species-dependent sensitivity (Atef et al., 2015). Likewise, PVA-based composite films loaded with black pepper or ginger essential oils significantly inhibited the growth of *Bacillus cereus*, *S. aureus*, *E. coli*, and *Salmonella typhimurium*, confirming that incorporation of essential oils into polymer films can provide broad antibacterial functionality (Amalraj et al., 2020). In another PVA-based system, Schinus molle essential oil-loaded PVA/gum Arabic hydrogels showed measurable inhibition zones against *S. aureus* and *Bacillus subtilis*, supporting the applicability of essential-oil-loaded PVA matrices for biomedical uses (Omoyeni & Kavaz, 2024).

It is generally accepted that Gram-negative bacteria are more resistant to essential oils because their outer membrane restricts the penetration of hydrophobic compounds, whereas Gram-positive bacteria are often more susceptible due to the absence of this barrier (Burt, 2004; Nazzaro et al., 2013). However, the present results deviated from this commonly reported trend, since no measurable inhibition zone was formed against *S. aureus*, while *E. coli* exhibited a clear response. This deviation may be attributed to the release behavior of the AMO components from the PVA/agar matrix rather than to bacterial cell-wall structure alone. At low AMO concentrations, β-cyclodextrin may retain a substantial fraction of the hydrophobic essential oil compounds within inclusion complexes, thereby reducing the amount of free active molecules able to diffuse into the agar medium. In addition, diffusion of the released compounds may be further restricted by the polymer network. At higher AMO loadings, partial saturation of β-cyclodextrin inclusion sites and an increased free-oil fraction may have promoted greater diffusion of active compounds, leading to the larger inhibition zones observed for PA-AMO2 and PA-AMO5. A similar dependence of antibacterial performance on concentration, composition, and release characteristics has been reported for essential oil systems in which the antimicrobial effect was not strictly concentration-dependent or varied according to oil composition and source (Galgano et al., 2022; Neagu et al., 2023).

Overall, the results demonstrate that AMO-containing PVA/agar films possess antibacterial activity primarily against *E. coli*, and that this activity is governed not only by essential oil concentration but also by matrix-controlled release and β-cyclodextrin-assisted encapsulation. The formation of inhibition zones confirms the release of active constituents from the films and supports their potential use as antibacterial wound dressing materials, although further studies are needed to clarify the release kinetics and to evaluate their activity with a broader microbiological panel.

3.5. Mechanical properties of the films

Film thickness, tensile strength (TS), elongation at break (EAB), and young's modulus (YM) values of the films were determined (Table 3). The reference PA film exhibited a TS of 6.35 ± 1.30 MPa, an EAB of 572.15 ± 81.48%, and a YM of 1.34 ± 0.44 MPa, which are consistent with the ranges reported in the literature for typical PVA/Agar based films (Pereira et al., 2013). Similarly, Madera-Santana et al. (2014) (Madera-Santana et al., 2014) reported tensile strength values of 5–10 MPa and elongation in the range of 400–550% for PVA/Agar films, further demonstrating that the presence of glycerol increases chain mobility and enhances flexibility.

YM values ranged between 0.83 and 2.29 MPa. Compared to the reference, PA-AMO0.5 (2.29 ± 0.68 MPa) and PA-AMO1 (2.19 ± 0.26 MPa) showed higher rigidity. This could be attributed to the addition of AML essential oil and β-CD, which enhanced intermolecular interactions among polymer chains, resulting in a stiffer structure. In line with this, Qian et al. (2022) reported significant increases in modulus and tensile strength in PVA-based composites containing β-CD, while Chen et al. (2020) showed that encapsulated AMO/β-CD systems improved stiffness at low concentrations but led to decreased (Chen et al., 2020; Qian et al., 2022) Young's modulus at high loadings due to phase separation. Consistently, PA-AMO5 (0.83 ± 0.66 MPa), with the highest oil content, showed the lowest YM value, indicating that excessive oil disrupted chain alignment and yielded a looser matrix.

EAB values ranged from 411.02% to 719.02%. The reference PA film showed 572.15% elongation. PA-AMO0.5 (628.83 ± 20.14%) and especially PA-AMO1 (719.02 ± 4.88%) exhibited greater flexibility, suggesting that the combined addition of AMO, β-CD, and glycerol enhanced chain mobility and phase compatibility at optimal levels.

Table 3. Mechanical properties and thickness values of the films.

Sample ID	Film thickness (µm)	YM* (MPa)	EAB* (%)	TS* (MPa)
PA	0.32	1.34 ± 0.44[a,b]	572.15 ± 81.48[b,c]	6.35 ± 1.30[a]
PA-AMO0.5	0.30	2.29 ± 0.68[b]	628.83 ± 20.14[c,d]	7.87 ± 0.76[a,b]
PA-AMO1	0.32	2.19 ± 0.26[b]	719.02 ± 4.88[d]	11.26 ± 0.04[b]
PA-AMO2	0.33	1.86 ± 0.13[a,b]	489.14 ± 32.52[a,b]	5.48 ± 2.07[a]
PA-AMO5	0.43	0.83 ± 0.66[a]	411.02 ± 48.18[a]	4.31 ± 0.81[a]

* Different superscript letters within the same column indicate statistically significant differences ($p < 0.05$).

A similar trend was observed by Šuput et al. (2016), who reported that low EO contents increased elongation at break in starch-based films, whereas higher EO concentrations reduced TS and diminished the effect on EAB. In line with a comprehensive review, increasing EO concentration weakens cohesion between polymer chains and promotes heterogeneity, leading to a decrease in EAB (Syafiq et al., 2020). Accordingly, higher oil-loaded films PA-AMO2 (489.14 ± 32.52%) and PA-AMO5 (411.02 ± 48.18%) exhibited significantly reduced elongation, which can be ascribed to heterogeneity and restricted chain mobility.

TS values were found in the range of 4.31–11.26 MPa. While the reference PA film had a TS of 6.35 ± 1.30 MPa, PA-AMO0.5 (7.87 ± 0.76 MPa) showed a slight improvement. The highest tensile strength was obtained for PA-AMO1 (11.26 ± 0.04 MPa). This increase can be associated with β-CD promoting hydrogen bonding and crosslinking interactions among polymer chains, thereby enhancing load-bearing capacity. PA-AMO2 (5.48 ± 2.07 MPa) and PA-AMO5 (4.31 ± 0.81 MPa) exhibited lower TS values compared to the reference, although these differences were not statistically significant ($p > 0.05$). These results suggest that AMO/β-CD addition at moderate levels enhances tensile properties, while excessive loading induces interfacial incompatibility and heterogeneity, leading to reduced strength without always reaching statistical significance (Valencia et al., 2019). Song et al. (2018) reported that the addition of lemon EO and surfactant to corn–wheat starch films markedly decreased TS, highlighting the potential of EO to compromise structural integrity (Song et al., 2018). Similarly, Syafiq et al. (2020) indicated that increasing EO content weakens chain cohesion and decreases tensile strength (Syafiq et al., 2020).

All obtained values fall within the recommended tensile strength range of 1–32 MPa for wound dressing materials (Yesilyurt et al., 2025), supporting the suitability of these films for biomedical applications. Overall, PA-AMO1 demonstrated the best mechanical performance with both high tensile strength and high elongation at break. This suggests that the optimal level of AMO and β-CD resulted in a well-balanced matrix structure, enhancing both strength and flexibility. In contrast, PA-AMO5 exhibited the weakest performance, with low TS and EAB values, likely due to inhomogeneous distribution and structural irregularities introduced by excessive oil and β-CD.

3.6. Color properties of the films

Color parameters (L*, a*, b*, ΔE, and yellowness index) are important indicators for evaluating the optical and structural properties of film-based wound dressing materials. These parameters provide information on film homogeneity, internal structure, and the dispersion of incorporated active agents such as essential oils. The incorporation of essential oils has been reported to alter color characteristics, particularly increasing yellowness due to the presence of bioactive compounds and changes in light interaction within the polymer matrix, reflecting variations in film composition and microstructure (Ribeiro-Santos et al., 2018; Venkatachalam et al., 2023). In addition, changes in L*, a*, b*, and ΔE values are commonly used to monitor formulation-dependent structural differences and interactions between polymer components and additives (Wang et al., 2022). The color parameters of the wound healing films are presented in Table 4. Examination of the L values revealed that the highest brightness was obtained for the PA film (99.06). As the concentration of essential oil increased, the L values gradually decreased, with the lowest value recorded for the PA-AMO5 film (94.32). Although these differences were statistically significant, even an L value of 94 represents a relatively high brightness, indicating that the films overall retained their light/semi-transparent character. In the literature, materials are considered transparent or translucent when their L values exceed 90 (Pathare et al., 2012; Jridi et al., 2014). This suggests that the inherent transparency of the PVA matrix was largely maintained, while the addition of essential oil and β-CD rendered the films only slightly more opaque. Similarly, Haghighi et al. (2021) reported that although the addition of additives decreased the L values of gelatin/PVA-based nanocomposite films, high transparency was preserved (Haghighi et al., 2021).

Regarding the a values, it was observed that films shifted toward green tones as the concentration of essential oil increased. PA and PA-AMO0.5 films, with statistically similar and low a values, exhibited the least color shift, whereas PA-AMO2 and PA-AMO5 films showed more negative values and were significantly different from the other groups. This finding indicates that the increased essential oil content altered the color balance of the matrix, shifting the films toward the green region.

Table 4. Color parameters of PVA/Agar based films enriched with *Achillea millefolium* L. essential oil.

Sample ID	L	a	b	ΔE	YI
PA	99.06 ± 0.17^{a}	-0.15 ± 0.01^{a}	0.57 ± 0.14^{a}	0.93 ± 0.19^{a}	0.83 ± 0.21^{a}
PA-AMO0.5	96.97 ± 0.32^{b}	-0.37 ± 0.05^{a}	$1.64 \pm 0.13^{a,b}$	3.19 ± 0.32^{b}	$2.42 \pm 0.20^{a,b}$
PA-AMO1	$95.98 \pm 0.42^{b,c}$	-0.83 ± 0.09^{a}	2.55 ± 0.19^{b}	4.58 ± 0.48^{b}	3.80 ± 0.50^{b}
PA-AMO2	$94.73 \pm 0.54^{c,d}$	-2.26 ± 0.27^{b}	5.54 ± 0.59^{d}	7.81 ± 0.81^{c}	8.37 ± 0.93^{c}
PA-AMO5	94.32 ± 0.91^{d}	-4.31 ± 0.51^{c}	8.56 ± 0.69^{e}	11.05 ± 1.17^{d}	12.97 ± 1.18^{d}

* Values indicated with different superscript letters within the same column represent statistically significant differences ($p < 0.05$).

In terms of b values, the highest value was obtained for the PA-AMO5 film (8.56). During the production of AMO (at high temperatures >100 °C), the compound matricin is decomposed into chamazulene, imparting a blue color to the oil. However, under the film preparation conditions (25 °C), this pigment was present only in small amounts, while the oil droplets were encapsulated by β-CD, leading to homogeneous dispersion within the matrix and increased opacity. Consequently, the blue tone was suppressed and yellow tones became more pronounced. The yellowness index also increased consistently with the b values. Previous studies have reported that β-CD enhances the homogeneous distribution of essential oil constituents within the polymer matrix, slows oxidative degradation, and improves color stability (López-Nicolás & García-Carmona, 2010; Recio-Cázares et al., 2024). In this context, the observed increase in both b values and YI with higher oil content can be attributed to the natural tones of the oil in combination with the encapsulation effect of β-CD. Notably, PA-AMO2 and PA-AMO5 films exhibited significantly higher YI values compared to the control group. These findings demonstrate that the incorporation of AMO induced a shift of the films toward yellowish tones.

The ΔE values increased gradually with higher essential oil concentrations. While the reference PA film exhibited the lowest ΔE value, remaining nearly indistinguishable from the control, the PA-AMO2 film showed a ΔE ≈ 7.81, corresponding to a moderate, perceptible color change. The highest ΔE value was recorded for the PA-AMO5 film (≈11). According to the literature, ΔE values above 5 indicate a clear color difference, whereas values above 10 signify a change that is easily perceptible to the naked eye (Pathare et al., 2012). Therefore, the elevated ΔE of the PA-AMO5 film reflects a distinct color change compared to the reference.

Overall, the incorporation of increasing amounts of AMO into the PA matrix led to reduced lightness, increased greenness, elevated yellowness, and significantly higher total color difference. At higher incorporation levels (PA-AMO2 and PA-AMO5), these changes in color parameters were statistically significant ($p < 0.05$), confirming that essential oil addition strongly influenced the optical properties of the films.

3. Conclusions

In this study, biodegradable PVA/Agar based films were prepared using a Pickering emulsion approach, and it was demonstrated that the essential oil of *Achillea millefolium* L. could be effectively stabilized within the polymer matrix with the aid of β-cyclodextrin. Structural analyses revealed no evidence of new covalent bond formation in the polymer backbone, but indicated that hydrogen bonding interactions were strengthened in the presence of AMO/β-CD. SEM micrographs confirmed the morphological transition from a smooth to a heterogeneous droplet-like structure with increasing oil content, serving as visual evidence of emulsion phase separation.

Mechanical testing showed that low levels of AMO/β-CD incorporation (particularly PA-AMO1) achieved an optimal balance by simultaneously enhancing tensile strength and elongation at break, while excessive loadings disrupted chain regularity and resulted in losses of both strength and flexibility. Colorimetric analyses revealed a slight decrease in L values, a consistent increase in b values and yellowness index, and a significant rise in ΔE with increasing oil concentration. Contact angle measurements indicated that the additives rendered the film surface more hydrophobic; however, all films remained below 90°, thereby retaining a hydrophilic character favorable for wound healing. Antibacterial assays demonstrated that neat PVA/Agar films showed no measurable inhibition zones, while AMO-loaded films exhibited concentration-dependent activity exclusively against *E. coli* (up to 18.5 mm at 5% AMO), with no detectable zones observed against *S. aureus*.

In summary, PVA/Agar films incorporating low-to-moderate levels of AMO/β-CD complexes displayed optimal mechanical performance, maintained hydrophilic surfaces, exhibited controlled color properties, and demonstrated antibacterial activity selectively against *E. coli*. These findings highlight the strong potential of such films as wound dressing candidates and underscore the promise of β-cyclodextrin assisted encapsulation of plant-derived essential oils as a strategy for the functional enhancement of biopolymer-based wound care materials.

Acknowledgement

The authors gratefully acknowledge Naile Angin (Faculty of Forestry) for her assistance with colorimetric tests and Ahmet Aydın (Department of Polymer Materials Engineering) for his support in mechanical testing. This work was supported by the Scientific and Technological Research Council of Türkiye (TÜBİTAK - Project No: 1919B012453915). The authors would also like to thank the editor and the reviewers for their valuable contributions during the evaluation of the manuscript.

Author contribution

All authors contributed equally to the conception, experimental design, data analysis, and preparation of the manuscript.

Declaration of ethical code

The authors of this article declare that the materials and methods used in this study do not require ethics committee approval and/or legal-special permission.

Conflicts of interest

The authors declare that there is no conflict of interest.

References

Abdul Khalil, H. P. S., Lai, T. K., Tye, Y. Y., Rizal, S., Chong, E. W. N., Yap, S. W., Hamzah, A. A., Nurul Fazita, M. R., & Paridah, M. T. (2018). A review of extractions of seaweed hydrocolloids: properties and applications. *Express Polymer Letters*, *12*(4), 296-317. https://doi.org/10.3144/expresspolymlett.2018.27

Ali, S. I., Gopalakrishnan, B., & Venkatesalu, V. (2017). Pharmacognosy, Phytochemistry and pharmacological properties of achillea millefolium L.: a review. *Phytotherapy Research*, *31*(8), 1140-1161. https://doi.org/10.1002/ptr.5840

Almasi, H., Azizi, S., & Amjadi, S. (2020). Development and characterization of pectin films activated by nanoemulsion and pickering emulsion stabilized marjoram (origanum majorana L.) essential oil. *Food Hydrocolloids*, *99*. https://doi.org/10.1016/j.foodhyd.2019.105338

Arham, R., Mulyati, M.T., Metusalach, M., Salengke, S. (2016). Physical and mechanical properties of agar based edible film with glycerol plasticizer. *International Food Research Journal*, *23*(4).

Atef, M., Rezaei, M., & Behrooz, R. (2015). Characterization of physical, mechanical, and antibacterial properties of agar-cellulose bionanocomposite films incorporated with savory essential oil. *Food Hydrocolloids*, *45*, 150–157. https://doi.org/10.1016/j.foodhyd.2014.09.037

Athamneh, T., Hajnal, A., Al-Najjar, M. A. A., Alshweiat, A., Obaidat, R., Awad, A. A., Al-Alwany, R., Keitel, J., Wu, D., Kieserling, H., Rohn, S., Keil, C., & Gurikov, P. (2023). In vivo tests of a novel wound dressing based on agar aerogel. I*nternational Journal of Biological Macromolecules*, *239*, 124238. https://doi.org/10.1016/j.ijbiomac.2023.124238

Baladi, F., & Sherafat, Z. (2025). Preparation and characterization of PVA/TA/TiO2 hydrogel films potentially applicable for wound dressings. *Materials Research Bulletin*, *191*. https://doi.org/10.1016/j.materresbull.2025.113555

Becker, L. C., Bergfeld, W. F., Belsito, D. V., Hill, R. A., Klaassen, C. D., Liebler, D. C., Marks, J. G., Jr., Shank, R. C., Slaga, T. J., Snyder, P. W., & Andersen, F. A. (2016). Safety assessment of achillea millefolium as used in cosmetics. *International Journal of Toxicology*, *35*(3 suppl), 5S-15S. https://doi.org/10.1177/1091581816677717

Blackburn, J., Kopecki, Z., & Ousey, K. J. (2024). Skin integrity, antimicrobial stewardship and infection control: a critical review of current best practice. *Wound Practice and Research*, *32*(1), 34–43. https://doi.org/10.33235/wpr.32.1.34-43

Brumberg, V., Astrelina, T., Malivanova, T., & Samoilov, A. (2021). Modern wound dressings: Hydrogel dressings. *Biomedicines*, *9*(9). https://doi.org/10.3390/biomedicines9091235

Buriti, B., Figueiredo, P. L. B., Passos, M. F., & da Silva, J. K. R. (2024). Polymer-based wound dressings loaded with essential oil for the treatment of wounds: a review. *Pharmaceuticals (Basel)*, *17*(7). https://doi.org/10.3390/ph17070897

Burt, S. (2004). Essential oils: their antibacterial properties and potential applications in foods-a review. *International Journal of Food Microbiology*, *94*(3), 223-253. https://doi.org/10.1016/j.ijfoodmicro.2004.03.022

Cao, L., Shao, G., Ren, F., Yang, M., Nie, Y., Peng, Q., & Zhang, P. (2021). Cerium oxide nanoparticle-loaded polyvinyl alcohol nanogels delivery for wound healing care systems on surgery. *Drug Delivery*, *28*(1), 390-399. https://doi.org/10.1080/10717544.2020.1858998

Cavallo, I., Sivori, F., Mastrofrancesco, A., Abril, E., Pontone, M., Di Domenico, E. G., & Pimpinelli, F. (2024). Bacterial biofilm in chronic wounds and possible therapeutic approaches. *Biology*, *13*(2), 109. https://doi.org/10.3390/biology13020109

Chen, K., Chen, G., Wei, S., Yang, X., Zhang, D., & Xu, L. (2018). Preparation and property of high strength and low friction PVA-HA/PAA composite hydrogel using annealing treatment. *Materials Science and Engineering: C*, *91*, 579-588. https://doi.org/10.1016/j.msec.2018.05.080

Chen, Q., Wu, J., Liu, Y., Li, Y., Zhang, C., Qi, W., Yeung, K. W. K., Wong, T. M., Zhao, X., & Pan, H. (2019). Electrospun chitosan/PVA/bioglass nanofibrous membrane with spatially designed structure for accelerating chronic wound healing. *Materials Science and Engineering: C*, *105*, 110083. https://doi.org/10.1016/j.msec.2019.110083

Chen, Z., Zong, L., Chen, C., & Xie, J. (2020). Development and characterization of PVA-starch active films incorporated with β-cyclodextrin inclusion complex embedding lemongrass (Cymbopogon citratus) oil. *Food Packaging and Shelf Life*, *26*. https://doi.org/10.1016/j.fpsl.2020.100565

Czech, K., Gawel-Beben, K., Szopa, A., Kukula-Koch, W., Jakschitz, T., Bonn, G., Hussain, S., Kubica, P., Ekiert, H., & Glowniak, K. (2023). Phytochemical profiling, antioxidant and tyrosinase regulatory activities of extracts from herb, leaf and ın vitro culture of achillea millefolium (Yarrow). *Molecules*, *28*(12). https://doi.org/10.3390/molecules28124791

Egri, O., & Erdemir, N. (2019). Production of hypericum perforatum oil-loaded membranes for wound dressing material and in vitro tests. *Artificial Cells, Nanomedicine, and Biotechnology*, *47*(1), 1404-1415. https://doi.org/10.1080/21691401.2019.1596933

El-Aassar, M. R., Ibrahim, O. M., Fouda, M. M. G., El-Beheri, N. G., & Agwa, M. M. (2020). Wound healing of nanofiber comprising polygalacturonic/hyaluronic acid embedded silver nanoparticles: In-vitro and in-vivo studies. *Carbohydrate Polymers*, *238*. https://doi.org/10.1016/j.carbpol.2020.116175

Fang, H., Wang, J., Li, L., Xu, L., Wu, Y., Wang, Y., Fei, X., Tian, J., & Li, Y. (2019). A novel high-strength poly(ionic liquid)/PVA hydrogel dressing for antibacterial applications. *Chemical Engineering Journal*, *365*, 153–164. https://doi.org/10.1016/j.cej.2019.02.030

Farhadi, N., Babaei, K., Farsaraei, S., Moghaddam, M., & Ghasemi Pirbalouti, A. (2020). Changes in essential oil compositions, total phenol, flavonoids and antioxidant capacity of Achillea millefolium at different growth stages. *Industrial Crops and Products*, *152*, 112570. https://doi.org/10.1016/j.indcrop.2020.112570

Feng, X., Hou, X., Cui, C., Sun, S., Sadik, S., Wu, S., & Zhou, F. (2021). Mechanical and antibacterial properties of tannic acid-encapsulated carboxymethyl chitosan/polyvinyl alcohol hydrogels. *Engineered Regeneration*, *2*, 57-62. https://doi.org/10.1016/j.engreg.2021.05.002

Fernando, I. P. S., Sanjeewa, K. K. A., Samarakoon, K. W., Lee, W. W., Kim, H.-S., Kim, E.-A., Gunasekara, U. K. D. S. S., Abeytunga, D. T. U., Nanayakkara, C., de Silva, E. D., Lee, H.-S., & Jeon, Y.-J. (2017). FTIR characterization and antioxidant activity of water soluble crude polysaccharides of Sri Lankan marine algae. *Algae*, *32*(1), 75-86. https://doi.org/10.4490/algae.2017.32.12.1

Galgano, M., Capozza, P., Pellegrini, F., Cordisco, M., Sposato, A., Sblano, S., Camero, M., Lanave, G., Fracchiolla, G., Corrente, M., Cirone, F., Trotta, A., Tempesta, M., Buonavoglia, D., & Pratelli, A. (2022). Antimicrobial activity of essential oils evaluated in vitro against Escherichia coli and Staphylococcus aureus. *Antibiotics*, *11*(7), 979. https://doi.org/10.3390/antibiotics11070979

Gasperini, L., Mano, J. F., & Reis, R. L. (2014). Natural polymers for the microencapsulation of cells. *Journal of the Royal Society Interface*, *11*(100), 20140817. https://doi.org/10.1098/rsif.2014.0817

Gioele, C., Marilena, S., Valbona, A., Nunziacarla, S., Andrea, S., & Antonio, M. (2017). Gracilaria gracilis, source of agar: A short review. *Current Organic Chemistry*, *21*(5), 380-386. https://doi.org/10.2174/1385272820666161017164605

Giulio Fittolani, P. H. S., Martina Delbianco. (2019). Helical polysaccharides. *Peptide Science*, *112*(1). https://doi.org/10.1002/pep2.24124

Gu, L., Sun, X., Pan, J., Liu, D., Huang, L., Yu, Y., Yu, B., & Cong, H. (2025). AIE-active PVA/berberine antibacterial hydrogel for wound healing, visual monitoring pH and dehydration. *Biomaterials*, *323*, 123432. https://doi.org/10.1016/j.biomaterials.2025.123432

Haghighi, H., Gullo, M., La China, S., Pfeifer, F., Siesler, H. W., Licciardello, F., & Pulvirenti, A. (2021). Characterization of bio-nanocomposite films based on gelatin/polyvinyl alcohol blend reinforced with bacterial cellulose nanowhiskers for food packaging applications. *Food Hydrocolloids*, *113*. https://doi.org/10.1016/j.foodhyd.2020.106454

Jin, S. G. (2022). Production and application of biomaterials based on polyvinyl alcohol (PVA) as wound dressing. *Chemistry – An Asian Journal*, *17*(21), e202200595. https://doi.org/10.1002/asia.202200595

Jridi, M., Hajji, S., Ayed, H. B., Lassoued, I., Mbarek, A., Kammoun, M., Souissi, N., & Nasri, M. (2014). Physical, structural, antioxidant and antimicrobial properties of gelatin-chitosan composite edible films. *International Journal of Biological Macromolecules*, *67*, 373-379. https://doi.org/10.1016/j.ijbiomac.2014.03.054

Ike, K., Omaliko, P., Fernander, M., Sanders, B., Enikuomehin, J., Alabi, J., Adelusi, O., Kholif, A., Thomas, M., & Anele, U. (2025). Evaluating the effect of an essential oil blend on the growth and fitness of gram-positive and gram-negative bacteria. *Biology*, *14*(4), 437. https://doi.org/10.3390/biology14040437

Karami, P., Zandi, M., & Ganjloo, A. (2022). Evaluation of physicochemical, mechanical, and antimicrobial properties of gelatin-sodium alginate-yarrow (achillea millefolium L.) essential oil film. *Journal of Food Processing and Preservation*, *46*(7). https://doi.org/10.1111/jfpp.16632

Kharat, Z., Amiri Goushki, M., Sarvian, N., Asad, S., Dehghan, M. M., & Kabiri, M. (2021). Chitosan/PEO nanofibers containing calendula officinalis extract: Preparation, characterization, in vitro and in vivo evaluation for wound healing applications. *International Journal of Pharmaceutics*, *609*, 121132. https://doi.org/10.1016/j.ijpharm.2021.121132

Khorasani, M. T., Joorabloo, A., Adeli, H., Milan, P. B., & Amoupour, M. (2021). Enhanced antimicrobial and full-thickness wound healing efficiency of hydrogels loaded with heparinized ZnO nanoparticles: In vitro and in vivo evaluation. *International Journal of Biological Macromolecules*, *166*, 200-212. https://doi.org/10.1016/j.ijbiomac.2020.10.142

Lei, S., Qin, X., Shen, S., Ma, X., Yang, C., Mai, X., Cao, X., Liu, Z., Xie, W., Yang, S., & Wang, J. (2025). Green synthesis of PVA-LS-MXene composite conductive hydrogel for high-performance skin wound dressings. *Journal of the Mechanical Behavior of Biomedical Materials*, *170*, 107107. https://doi.org/10.1016/j.jmbbm.2025.107107

Li, X., Yang, X., Wang, Z., Liu, Y., Guo, J., Zhu, Y., Shao, J., Li, J., Wang, L., & Wang, K. (2022). Antibacterial, antioxidant and biocompatible nanosized quercetin-PVA xerogel films for wound dressing. *Colloids and Surfaces B: Biointerfaces*, *209*, 112175. https://doi.org/10.1016/j.colsurfb.2021.112175

Liang, X., Zhong, H. J., Ding, H., Yu, B., Ma, X., Liu, X., Chong, C. M., & He, J. (2024). Polyvinyl alcohol (PVA)-based hydrogels: Recent progress in fabrication, properties, and multifunctional applications. *Polymers*, *16*(19). https://doi.org/10.3390/polym16192755

Liu, Q.-R., Wang, W., Qi, J., Huang, Q., & Xiao, J. (2019). Oregano essential oil loaded soybean polysaccharide films: Effect of pickering type immobilization on physical and antimicrobial properties. *Food Hydrocolloids*, *87*, 165-172. https://doi.org/10.1016/j.foodhyd.2018.08.011

Lohakan, M., Jamnongkan, T., Pintavirooj, C., Kaewpirom, S., & Boonsang, S. (2010). A numerical model for ultrasonic measurements of swelling and mechanical properties of a swollen PVA hydrogel. *Ultrasonics*, *50*(8), 782-789. https://doi.org/10.1016/j.ultras.2010.03.005

López-Nicolás, J. M., & García-Carmona, F. (2010). Effect of hydroxypropyl-β-cyclodextrin on the aggregation of (E)-resveratrol in different protonation states of the guest molecule. *Food Chemistry*, *118*(3), 648-655. https://doi.org/10.1016/j.foodchem.2009.05.039

Madera-Santana, T. J., Freile-Pelegrin, Y., & Azamar-Barrios, J. A. (2014). Physicochemical and morphological properties of plasticized poly(vinyl alcohol)-agar biodegradable films. *International Journal of Biological Macromolecules*, *69*, 176-184. https://doi.org/10.1016/j.ijbiomac.2014.05.044

Mansur, H. S., Sadahira, C. M., Souza, A. N., & Mansur, A. A. P. (2008). FTIR spectroscopy characterization of poly (vinyl alcohol) hydrogel with different hydrolysis degree and chemically crosslinked with glutaraldehyde. *Materials Science and Engineering: C*, *28*(4), 539-548. https://doi.org/10.1016/j.msec.2007.10.088

Martin, P. (1997). Wound healing-aiming for perfect skin regeneration. *Science, 276*(5309), 75–81. https://doi.org/10.1126/science.276.5309.75

Mohammadhosseini, M., Sarker, S. D., & Akbarzadeh, A. (2017). Chemical composition of the essential oils and extracts of achillea species and their biological activities: A review. *Journal of Ethnopharmacology*, *199*, 257-315. https://doi.org/10.1016/j.jep.2017.02.010

Nazir, I., Gangoo, S.A., Sofi, P.A., & Singh, A. (2022). GC-MS Analysis and Antioxidant Activity of the Essential Oil from Flowers of Achillea millefolium L. Under Temperate Climatic Conditions of Kashmir. *Journal of Essential Oil Bearing Plants, 25*, 290–296. https://doi.org/10.1080/0972060X.2022.2083456

Nazzaro, F., Fratianni, F., De Martino, L., Coppola, R., & De Feo, V. (2013). Effect of essential oils on pathogenic bacteria. *Pharmaceuticals (Basel)*, *6*(12), 1451-1474. https://doi.org/10.3390/ph6121451

Neagu, R., Popovici, V., Ionescu, L., Ordeanu, V., Popescu, D., Ozon, E., & Gîrd, C. (2023). Antibacterial and antibiofilm effects of different samples of five commercially available essential oils. *Antibiotics*, *12*(7), 1191. https://doi.org/10.3390/antibiotics12071191

Negut, I., Grumezescu, V., & Grumezescu, A. M. (2018). Treatment strategies for infected wounds. *Molecules*, *23*(9). https://doi.org/10.3390/molecules23092392

Pathare, P. B., Opara, U. L., & Al-Said, F. A.-J. (2012). Colour measurement and analysis in fresh and processed foods: A review. *Food and Bioprocess Technology*, *6*(1), 36-60. https://doi.org/10.1007/s11947-012-0867-9

Pereira, R., Carvalho, A., Vaz, D. C., Gil, M. H., Mendes, A., & Bartolo, P. (2013). Development of novel alginate based hydrogel films for wound healing applications. *International Journal of Biological Macromolecules*, *52*, 221-230. https://doi.org/10.1016/j.ijbiomac.2012.09.031

Pérez-Nava, A., Espino-Saldaña, A. E., Pereida-Jaramillo, E., Hernández-Vargas, J., Martínez-Torres, A., Vázquez-Lepe, M. O., Mota-Morales, J. D., Frontana Uribe, B. A., & Betzabe González-Campos, J. (2023). Surface collagen functionalization of electrospun poly(vinyl alcohol) scaffold for tissue engineering. *Process Biochemistry*, *126*, 1-14. https://doi.org/10.1016/j.procbio.2022.12.022

Pham, B.-T. T., Duong, T.-H. T., Nguyen, T. T., Van Nguyen, D., Trinh, C. D., & Bach, L. G. (2021). Development of polyvinyl (alcohol)/D-glucose/agar/silver nanoparticles nanocomposite film as potential food packaging material. *Journal of Polymer Research*, *28*(11). https://doi.org/10.1007/s10965-021-02761-1

Qian, Z. J., Zhang, J., Xu, W. R., & Zhang, Y. C. (2022). Development of active packaging films based on liquefied shrimp shell chitin and polyvinyl alcohol containing beta-cyclodextrin/cinnamaldehyde inclusion. *International Journal of Biological Macromolecules*, *214*, 67-76. https://doi.org/10.1016/j.ijbiomac.2022.06.052

Omoyeni, T. M., & Kavaz, D. (2024). Phytochemical screening of an essential oil-loaded PVA/GA hydrogel membrane for potential wound healing applications. *International Journal of Biological Macromolecules*, *283*, 137711. https://doi.org/10.1016/j.ijbiomac.2024.137711

Peña, O. A., & Martin, P. (2024). Cellular and molecular mechanisms of skin wound healing. *Nature Reviews Molecular Cell Biology*, *25*, 599–616. https://doi.org/10.1038/s41580-024-00715-1

Pulaj, B., Mustafa, B., & Hajdari, A. (2024). Differentiation of Achillea millefolium, A. crithmifolia, and A. nobilis through Analysis of Volatile Constituents using HS-SPME-GC/MS and Chemometric Techniques. *Records of Natural Products*, *18*, https://doi.org/10.25135/rnp.482.2408.3286

Recio-Cázares, S. L., Comett-Figueroa, P. I., Navarro-Amador, R., López-Malo, A., & Palou, E. (2024). β-Cyclodextrin ınclusion complex with essential oil from lippia (aloysia citriodora): Preparation, physicochemical characterization, and ıts application on beef. *ACS Food Science & Technology*, *4*(12), 3076-3087. https://doi.org/10.1021/acsfoodscitech.4c00654

Reddy, J. P., & Rhim, J. W. (2014). Characterization of bionanocomposite films prepared with agar and paper-mulberry pulp nanocellulose. *Carbohydrate Polymers*, *110*, 480-488. https://doi.org/10.1016/j.carbpol.2014.04.056

Ribeiro-Santos, R., Melo, N. R., Andrade, M., Azevedo, G., Machado, A. V., Carvalho-Costa, D., & Sanches-Silva, A., 2018. Whey protein active films incorporated with a blend of essential oils: Characterization and effectiveness. *Packaging Technology and Science*, *31*, 27–40. https://doi.org/10.1002/pts.2352

Russo, B., Brembilla, N. C., & Chizzolini, C. (2020). Interplay between keratinocytes and fibroblasts: A systematic review providing a new angle for understanding skin fibrotic disorders. *Frontiers in Immunology*, *11*, 648. https://doi.org/10.3389/fimmu.2020.00648

Sang Su Ha, E. S. S., Ping Du, Muhammad Suhaeri, Jong Ho Lee, Kwideok Park. (2020). A novel ECM patch combines polyvinyl alcohol, human fibroblast-derived matrix and mesenchymal stem cells for advanced wound healing. *ACS Biomaterials Science & Engineering,*, *6*(7).

Song, X., Zuo, G., & Chen, F. (2018). Effect of essential oil and surfactant on the physical and antimicrobial properties of corn and wheat starch films. *International Journal of Biological Macromolecules*, *107*(Pt A), 1302-1309. https://doi.org/10.1016/j.ijbiomac.2017.09.114

Stojanovic, G., Radulovic, N., Hashimoto, T., & Palic, R. (2005). In vitro antimicrobial activity of extracts of four achillea species: The composition of achillea clavennae L. (asteraceae) extract. *Journal of Ethnopharmacology*, *101*(1-3), 185-190. https://doi.org/10.1016/j.jep.2005.04.026

Strzepek-Gomolka, M., Gawel-Beben, K., & Kukula-Koch, W. (2021). Achillea species as sources of active phytochemicals for dermatological and cosmetic applications. *Oxidative Medicine and Cellular Longevity*, *2021*, 6643827. https://doi.org/10.1155/2021/6643827

Šuput, D., Lazić, V., Pezo, L., Markov, S., Vaštag, Ž., Popović, L., Radulović, A., Ostojić, S., Zlatanović, S., & Popović, S. (2016). Characterization of starch edible films with different essential oils addition. *Polish Journal of Food and Nutrition Sciences*, *66*(4), 277-285. https://doi.org/10.1515/pjfns-2016-0008

Syafiq, R., Sapuan, S. M., Zuhri, M. Y. M., Ilyas, R. A., Nazrin, A., Sherwani, S. F. K., & Khalina, A. (2020). Antimicrobial activities of starch-based biopolymers and biocomposites ıncorporated with plant essential oils: A review. *Polymers*, *12*(10). https://doi.org/10.3390/polym12102403

Tavakoli, S., & Klar, A. S. (2020). Advanced hydrogels as wound dressings. *Biomolecules*, *10*(8). https://doi.org/10.3390/biom10081169

Tamer, M. T., Sabet, M. M., Omer, A. M., Abbas, E., Eid, A. I., Mohy-Eldin, M. S., & Hassan, M. A. (2021). Hemostatic and antibacterial PVA/kaolin composite sponges loaded with penicillin–streptomycin for wound dressing applications. *Scientific Reports*, *11*, 3428. https://doi.org/10.1038/s41598-021-82963-1

Teodorescu, M., Bercea, M., & Morariu, S. (2018). Biomaterials of poly(vinyl alcohol) and natural polymers. *Polymer Reviews*, *58*(2), 247-287. https://doi.org/10.1080/15583724.2017.1403928

Tuberoso, C.I.G., & Kowalczyk, A., (2009). Chemical Composition of the Essential Oils of Achillea millefolium L. Isolated by Different Distillation Methods. *Journal of Essential Oil Research*, *21*, https://doi.org/10.1080/10412905.2009.9700125

Tyeb, S., Kumar, N., Kumar, A., & Verma, V. (2018). Flexible agar-sericin hydrogel film dressing for chronic wounds. *Carbohydrate Polymers, 200*, 572-582. https://doi.org/10.1016/j.carbpol.2018.08.030

Uberoi, A., McCready-Vangi, A., & Grice, E. A. (2024). The wound microbiota: microbial mechanisms of impaired wound healing and infection. *Nature Reviews Microbiology*, *22*, 507–521. https://doi.org/10.1038/s41579-024-01035-z

Valencia, L., Nomena, E. M., Mathew, A. P., & Velikov, K. P. (2019). Biobased cellulose nanofibril-oil composite films for active edible barriers. *ACS Applied Materials & Interfaces*, *11*(17), 16040-16047. https://doi.org/10.1021/acsami.9b02649

Venkatachalam, K., Rakkapao, N., & Lekjing, S. (2023). Physicochemical and antimicrobial characterization of chitosan and native glutinous rice starch-based composite edible films*: Influence of different essential oils incorporation. Membranes*, *13*, 161. https://doi.org/10.3390/membranes13020161

Verma, R. S., Joshi, N., Padalia, R. C., Goswami, P., Singh, V. R., Chauhan, A., Verma, S. K., Iqbal, H., Verma, R. K., Chanda, D., Sundaresan, V., & Darokar, M. P. (2017). Chemical composition and allelopathic, antibacterial, antifungal and in vitro acetylcholinesterase inhibitory activities of yarrow (achillea millefolium L.) native to India. *Industrial Crops and Products*, *104*, 144-155. https://doi.org/10.1016/j.indcrop.2017.04.046

Vig, K., Chaudhari, A., Tripathi, S., Dixit, S., Sahu, R., Pillai, S., Dennis, V. A., & Singh, S. R. (2017). Advances in skin regeneration using tissue engineering. *International Journal of Molecular Sciences*, *18*(789). https://doi.org/10.3390/ijms18040789

Villalva, M., Silvan, J. M., Alarcon-Cavero, T., Villanueva-Bermejo, D., Jaime, L., Santoyo, S., & Martinez-Rodriguez, A. J. (2022). Antioxidant, anti-inflammatory, and antibacterial properties of an achillea millefolium l. extract and ıts fractions obtained by supercritical anti-solvent fractionation against helicobacter pylori. *Antioxidants (Basel)*, *11*(10). https://doi.org/10.3390/antiox11101849

Wang, B., Yan, S., Qiu, L., Gao, W., Kang, X., Yu, B., Liu, P., Cui, B., & Abd El-Aty, A. M. (2022). Antimicrobial activity, microstructure, mechanical, and barrier properties of cassava starch composite films supplemented with geranium essential oil. *Frontiers in Nutrition*, *9*, 882742. https://doi.org/10.3389/fnut.2022.882742

Wendy L. Applequist, D. E. M. (2011). Yarrow (achillea millefolium L.): A neglected panacea? a review of ethnobotany, bioactivity, and biomedical research. *Economic Botany*, *65*(2).

Xiang, C., Guo, Z., Zhang, Q., Wang, Z., Li, X., Chen, W., Wei, X., Li, P., & Xiang, C. (2024). Physically crosslinked poly(vinyl alcohol)-based hydrogels for cartilage tissue engineering. *Materials & Design*, *243*. https://doi.org/10.1016/j.matdes.2024.113048

Yan, Y., Li, M., Guo, L., Zhang, W., Wu, R., Guan, T., Ling, J., Yang, Y., Liu, M., Gu, X., & Liu, Y. (2025). Silk fibroin hydrogel with recombinant silk fibroin/NT3 protein enhances wound healing by promoting type III collagen synthesis and hair follicle regeneration in skin injury. *Mater Today Bio*, *33*, 101957. https://doi.org/10.1016/j.mtbio.2025.101957

Yesilyurt, A. (2025). Development and characterization of PVA/KGM-based bioactive films incorporating natural extracts and thyme oil. *Polymers*, *17*(17). https://doi.org/10.3390/polym17172425

Yesilyurt, A., Mayakrishnan, G., Parin, U., Kim, I. S., Parin, F. N., & Ullah, A. (2025). Design and characterization of polyvinyl alcohol/kappa-carrageenan pickering emulsion biocomposite films for potential wound care applications. *Journal of Biomedical Materials Research Part A, 113*(1), e37850. https://doi.org/10.1002/jbm.a.37850

Yuan, T., Xu, Y., Wang, Y., Han, P., & Chen, J. (2018). A tilt receiver correction method for visible light positioning using machine learning method. *IEEE Photonics Journal*, *10*(6), 1-12. https://doi.org/10.1109/jphot.2018.2880872

Yuan, J., Wang, Y., Kang, X., Guo, C., ji, H., Wu, L., & Qin, Y. (2026). Smart pH-responsive hydrogels: A versatile tool for addressing public health challenges in diagnostic and therapeutic applications. *European Polymer Journal*, *242*. https://doi.org/10.1016/j.eurpolymj.2025.114466

Zhou, T., Chen, S., Ding, X., Hu, Z., Cen, L., & Zhang, X. (2021). Fabrication and characterization of collagen/PVA dual-layer membranes for periodontal bone regeneration. *Frontiers in Bioengineering and Biotechnology*, *9*, 630977. https://doi.org/10.3389/fbioe.2021.630977